Ballistic Electron Emission Spectroscopy on Biased GaAs-AlGaAs Superlattices in Transverse Magnetic Fields

D. Rakoczy, G. Strasser, J. Smoliner

**Institut für Festkörperelektronik, TU-Wien,
Floragasse 7, 1040 Wien, Austria**

In this work, we introduce a metal-insulator-metal (MIM) injector structure as a solid-state version of ballistic electron emission spectroscopy (BEES) and utilize this structure for the investigation of the lowest miniband of a biased GaAs-AlGaAs superlattice in a transverse magnetic field. The ballistic electron current measured as a function of the collector bias shows a peak at flatband condition indicating coherent transport through the superlattice miniband. With increasing transverse magnetic field, the coherent transport decreases, i.e. the peak is quenched. Using an extended transfer matrix method, the observed effects are explained quantitatively.

1. Introduction

Ballistic electron emission spectroscopy (BEES) is a method to probe metal-semiconductor interfaces as well as the band structure of semiconductor heterostructures. In the form of a three-terminal extension of scanning tunneling microscopy (STM) [1], [2], BEES was initially used to determine Schottky barrier heights [3] – [6]. Later BEES was also applied to study subsurface structures, such as buried GaAs-AlGaAs double barrier resonant tunneling diodes [7], superlattices [8], [9], and self-assembled InAs quantum dots [10], [11]. The main advantage of STM-based BEES is an excellent spatial resolution, which can also be used for imaging nanostructures with ballistic electrons (BEEM). However, in some experimental environments, e.g. high transverse magnetic fields or temperatures in the mK range, conventional STM equipment is difficult to use. To avoid these obstacles one can replace the STM tip by a solid-state injector which is directly integrated on the sample under investigation. As spatial resolution is usually not required for purely spectroscopic applications, device based BEES is a useful supplement to STM-based BEES. In the literature there are several reports on devices for BEES, such as hot electron transistors on the basis of GaAs–AlGaAs heterostructures [12] or the injector structures introduced by Rauch et al. [13]. Yet one has to keep in mind that all these experiments were carried out on highly specialized molecular beam epitaxy (MBE) grown structures and, in addition, required an advanced sample processing. Therefore, we were looking for a versatile, robust and easy-to-produce solid-state emitter for ballistic electrons. A very promising candidate is a metal-insulator-metal (MIM) injector based on Al–Al_2O_3–Al, which can be used on virtually any substrate material, provided the quality of the Schottky contact between the aluminum base layer and the semiconductor is good enough. The first MIM injector for ballistic electrons was realized on bulk germanium by Spratt et al. [14], whose device proved to be suitable for operation as a hot electron transistor. First tests of our MIM injector [15] were carried out on various heterostructures, which we had previously investigated with

STM-based BEES. After proving that this type of injector is a suitable tool for BEES, we applied it to a sample with a superlattice and investigated its behavior in a transverse magnetic field.

2. Sample Preparation and Experimental Setup

To test our new emitter concept we compared two different types of MBE-grown GaAs–AlGaAs samples. The first consisted of GaAs only, while the other one had a single, 10 nm thick AlGaAs barrier 30 nm below the surface. All samples (also the superlattices) were grown with a very thin region of highly p-doped GaAs ("δ-doping") in the otherwise nominally undoped GaAs to provide a "flatband" condition at the surface. The pattern of our injector structure was defined by optical lithography and is shown in Fig. 1(a). To process the MBE grown samples, first ohmic contacts to the n^+ collector region were established using a standard Ge–Au–Ni–Au metallization. Prior to the evaporation of the Al base layer, the native surface oxide was removed by dipping the samples in a 1:1 solution of HCl (35%) and de-ionized water. Then a 150 Å thick Al layer was evaporated onto the sample, which serves both as a base electrode and for the growth of the Al_2O_3 tunneling barrier. The base metallization was oxidized at ambient conditions (cleanroom environment) for 30 min at 50 °C to form a protective layer on the Al base layer for the subsequent lithography step. To fabricate the tunneling barrier, a second oxidation step of 3 min duration at 100 °C was carried out after the lithography for the emitter pattern. As a last step, a 600 Å thick Al emitter electrode was sputtered on top of the sample. For the measurements the samples were cooled down to T = 4.2 K and, in case of the superlattices, exposed to transverse magnetic fields of up to 8 T (see Fig. 1(b)). In the following, V_E denotes the voltage between emitter and base, I_t the corresponding tunneling current, and I_c the collector current. V_c, the bias voltage between base and collector, causes a tilt in the conduction band profile.

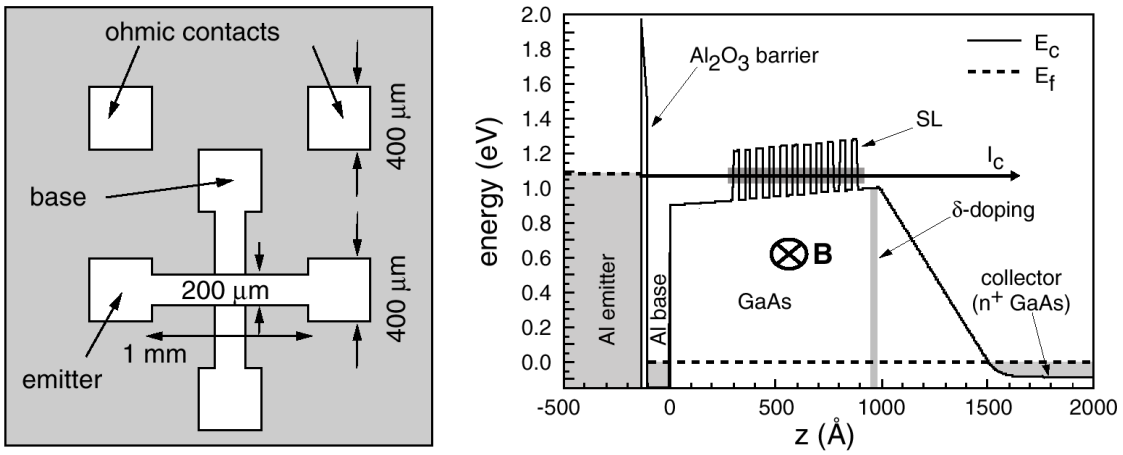

(a) (b)

Fig. 1: (a) Sample layout. (b) Schematic conduction band profile of our device applied to a sample with a superlattice. Below the AlGaAs barrier height only ballistic electrons with the proper energy to pass through the miniband (indicated by the gray area in the superlattice) contribute to the collector current I_c.

3. Experimental Results

For all samples the BEE spectra ($\alpha = I_c/I_t$ vs. V_E) show that the transfer ratio α is negligible up to a certain threshold in V_E and increases rapidly after this onset. The measured onset voltages agree very well with the values expected from the band profile parameters. For $V_c = 0$ V we obtain $V_{onset} = -0.803$ V for the sample without any barrier and $V_{onset} = -1.113$ V for the sample with one AlGaAs barrier [15]. The measured height of the AlGaAs barrier (i.e. the difference of the two onset voltages) is thus 310 meV, in good agreement with the results obtained by STM-based BEES on the same samples. The onset voltages and the shape of the BEE spectra were reproduced on several samples and also agree excellently with the calculated results. On the other hand the total amount of the ballistic current shows large deviations when measured on different samples. This seems to originate from variations of the quality of the Al_2O_3 barrier.

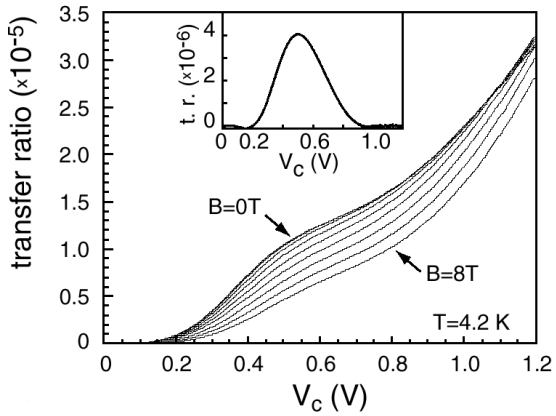

(a)

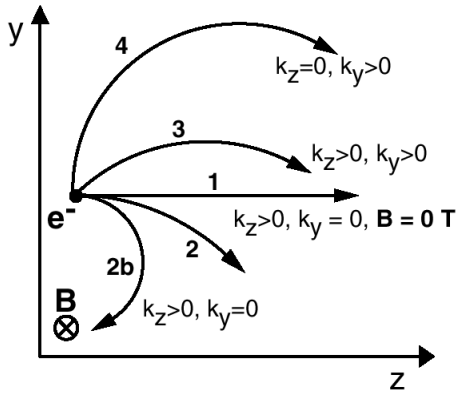

(b)

Fig. 2: (a) Measured transfer ratios vs. V_c for $V_E = -1.06$ V. The curves are measured at various B-fields from B = 0 T to 8 T in steps of 1 T (from left to right). At B = 0 T a peak at flatband condition is observed, which is quenched with increasing field. The inset shows the data for B = 0 T after background subtraction.
(b) Classical trajectories of electrons in a transverse magnetic field. Curve 1 shows a path without any B-field, the other trajectories are influenced by a B-field parallel to the x-axis. k_y, k_z denote the initial values of the momentum components. Curves 2 and 2b have identical initial momenta, but for 2b the B-field is higher.

Applying a positive voltage to the collector of the sample with the single barrier shifts the onset to smaller absolute values in V_E, just as expected from the band profile: $V_c > 0$ V means a lowering of the collector Fermi level which leads to a tilt of the band profile and therefore reduces the effective height of the AlGaAs barrier. The measured decrease in V_{onset} agrees very well with results from self-consistent calculations [15]. We also tested the behavior of the superlattice samples under bias before putting them into the magnetic field. These tests revealed that at zero bias the band structure of the superlattice is in fact slightly tilted, and an external collector voltage of $V_c \approx 500$ mV is needed to provide genuine flatband condition. This can also be seen directly in the measurement of the transfer ratio α in dependence of V_c for a constant emitter voltage (in the miniband regime, e.g. $V_E = -1.06$ V). After subtraction of a roughly exponential

background these curves exhibit a peak at flatband condition (see inset of Fig. 2(a)), indicating the transport through the miniband (the structure was designed in such a way that only one miniband exists below the AlGaAs barrier height). For flatband condition the onset voltage in the BEE spectra for this type of sample corresponds very well with the calculated lower edge of the miniband. A detailed description of the BEE spectra as well as a comparison with STM based BEES data can be found in [16].

The next step was to investigate the influence of the transverse magnetic field on the ballistic current. As one can already clearly see from the raw data in Fig. 2(a), the peak height in $\alpha(V_c)$ decreases with increasing magnetic field. This can already be explained by using the simple classical model of a charged particle in a transverse magnetic field (see Fig. 2(b)). The Lorentz force couples the k_y (parallel to the interface) and k_z (orthogonal to the interface) components of the electron momentum, whereas k_x, the component parallel to the B-field, stays unaffected. Due to the B-field, an electron can therefore lose k_z and gain k_y (and vice versa). Whether an electron is able to go through the superlattice or not depends on its kinetic energy associated with k_z, i.e. E_z. Electrons with an initial value of $k_y > 0$ can gain E_z via this mechanism, while all other electrons will always lose E_z. This diminishes the number of electrons with the right energy to pass the superlattice and leads to the observed change in the transmission.

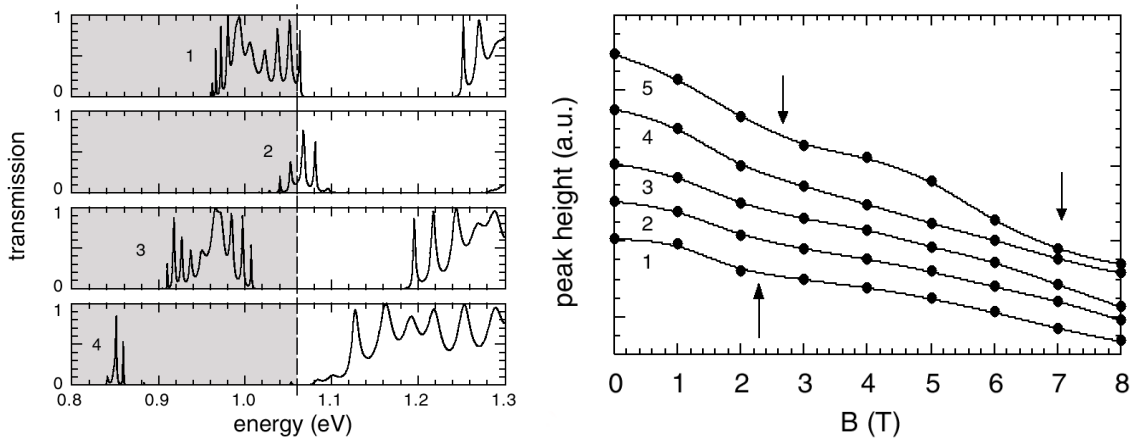

(a) (b)

Fig. 3: (a) Transmission coefficient of the superlattice for several parameter sets.
1: B = 0 T, E_y = 0 meV; **2**: B = 3 T, E_y = 0 meV; **3**: B = 3 T, E_y = 60 meV;
4: B = 8.2 T, E_y = 210 meV. The dashed line indicates the position of the Fermi energy in the emitter for V_E = –1.06 V.
(b) $\alpha(V_c)$ peak amplitude vs. B-field. The solid line is just a guide for the eye. Curves 1–5 correspond to V_E = –1.04, –1.05, –1.06, –1.07, and –1.08 V respectively. The phonon associated features are marked by arrows.

In the quantum mechanic treatment the B field results in an additional term in the Schrödinger equation, which can be treated as a magnetic field induced potential. With this, the transmission can be calculated using conventional transfer matrix methods [16]. Fig. 3(a) shows the transmission coefficient of our superlattice structure at flatband condition as a function of E_z, calculated for different magnetic fields and different initial values of k_y. Curve 1 was calculated for B = 0 T and $k_y = 0$. As one can see, the miniband is located between 0.96 and 1.07 eV. If B is increased the transmissive regime for

electrons with $k_y = 0$ is shifted to higher energy and becomes smaller (curve 2). However, in our experiment also electrons with positive and negative initial k_y values are injected. Electrons with $k_y < 0$ will be reflected back already at small B fields. On the other hand, electrons with positive k_y will gain E_z, which means that the transmissive range is shifted to lower values of E_z (curve 3). Despite this fact, more and more electrons are reflected back. Thus, the coherent current decreases, as it is observed experimentally. Curve 4 shows the situation for B = 8.2 T, E_y = 210 meV, and $E_z = V_b$, where V_b is the Schottky barrier height. Note that this is the highest possible E_y for V_E = -1.06 eV. For this case only a narrow transmission range exists just above V_b. If B is increased further (B > 8.5 T), the transmission is inhibited for all electrons below $e \cdot V_e$ = 1.06 eV.

Plotting the peak height in $\alpha(V_c)$ (after background subtraction, see inset in Fig. 2(a)) vs. B, we observe a decrease for all emitter voltages (see Fig. 3(b)). This decrease is not completely linear, but exhibits one or two kinks, which can be interpreted as a result of sequential LO-phonon emission inside the superlattice. Simple classical estimations show that without magnetic field, the electron transfer time through our superlattice structure (≈100 fs) is just somewhat smaller than the LO-phonon emission time (≈150 fs). In a transverse magnetic field, the transfer time increases, since the average z component of the electron velocity decreases. If the LO-phonon scattering time is exceeded, scattering will occur and the scattered electrons will no longer contribute to the coherent current. Thus, the peak amplitude decreases faster than normal. If B is increased further, a second scattering can occur, provided the electron energy is still high enough. The miniband is about 100 meV broad, therefore in principle allowing the emission of 3 phonons. At V_E = –1.08 V, where the Fermi energy in the emitter is approximately aligned with the top of the miniband, we see two kinks in the data, while for the other curves the second kink is not observable. The second peak at low emitter bias does probably not occur because at high B-field and low injection energy most of the electrons are already below the LO-phonon energy after the first scattering. The third peak is probably missing even at higher energies, since at 8 T the transfer time might still be too small for three sequential phonon emissions.

4. Conclusion

We have developed a MIM injector structure for BEES and used it to investigate the ballistic transport through a superlattice in a transverse magnetic field. We explained the observed behavior quantitatively with an extended transfer matrix method. Furthermore, indications for sequential LO-phonon scattering inside the superlattice, facilitated by the magnetic field via increased transfer times, can be observed.

Acknowledgements

This work was sponsored by the "*Fonds zur Förderung der wissenschaftlichen Forschung*" as project No. P12925-TPH and by the "*Gesellschaft für Mikroelektronik*".

References

[1] W. J. Kaiser and L. D. Bell, *Phys. Rev. Lett.*, **60**, 1406 (1988).

[2] L. D. Bell and W. J. Kaiser, *Phys. Rev. Lett.*, **61**, 2368 (1988).

[3] W. J. Kaiser et a.l., *Phys. Rev. B*, **48**, 18324 (1993).

[4] H. Sirringhaus, E. Y. Lee, and H. von Känel, *Phys. Rev. Lett.*, **73**,577 (1994).

[5] R. Ludeke, M. Prietsch, and A. Samsavar, *J. Vac. Sci. Technol. B*, **9**, 2342 (1991).

[6] M. Prietsch and R. Ludeke, *Phys. Rev. Lett.*, **66**, 2511 (1991).

[7] T. Sajoto et al., *Phys. Rev. Lett.*, **74**, 3427 (1995).

[8] J. Smoliner, R. Heer, C. Eder, and G. Strasser, *Phys. Rev. B*, **58**, 7516 (1998).

[9] R. Heer, J. Smoliner, G. Strasser, and E. Gornik, *Appl. Phys. Lett.*, **73**, 3138 (1998).

[10] M. E. Rubin et al., *Phys. Rev. Lett.*, **77**, 5268 (1996).

[11] W. Wu, J. R. Tucker, G. S. Solomon, J. S. Harris, Jr., *Appl. Phys. Lett.*, **71**, 1083 (1997).

[12] M. Heiblum et al., *Phys. Rev. Lett.*, **55**, 2200 (1985).

[13] C. Rauch et al., *Phys. Rev. Lett.*, **81**, 3495 (1998).

[14] J. P. Spratt, R. F. Schwarz, and W. M. Kane, *Phys. Rev. Lett.*, **6**, 341 (1961).

[15] R. Heer, et al., *Appl. Phys. Lett.*, **73**, 3138 (1998).

[16] D. Rakoczy, J. Smoliner, R. Heer, and G. Strasser, *J. Appl. Phys.*, **88**, 3495 (2000).